Journal of Cell Science & Therapy

Rajiah, J Cell Sci Ther 2013, 4:1
DOI: 10.4172/2157-7013.1000138

Research Article Open Access

PARP-1 N-Terminal Fragment Down-regulates Endogenous PARP-1 Expression and Activity and Sensitises Cells to Oxidative Stress

Ida Rachel Rajiah*

Department of Pathology, University of Cambridge, Tennis Court Road, Cambridge CB2 1QP, UK

Abstract

Poly (ADP-ribose) polymerase-1 (PARP-1) is a nuclear enzyme that plays a vital role in DNA repair. This makes it an attractive anticancer therapeutic target. It is activated by DNA breaks and catalyses the synthesis of homopolymers of ADP-ribose from NAD+. Competitive inhibitors as well as the non-catalytic, DNA-binding domain of PARP-1 abolish its polymer synthesising function. Inhibitors of PARP-1 have been used in clinical trials and are known to cause nausea, fatigue and haematological events and with chronic use the risk of drug-induced DNA damage and tumorigenesis. In this study, I have investigated the effect of PARP-1-N-terminal fragment on endogenous PARP-1 activity and expression in mammalian cells. To elicit DNA damage response, different concentrations of H_2O_2 were used. For visualisation of the effects by live imaging, 750 bp PARP-1-N-terminal fragment was tagged to enhanced green fluorescent protein (EGFP) vector. My data shows an inverse correlation between the expression of this fragment and poly (ADP-ribose) synthesis at lower concentrations of H_2O_2 and induction of apoptosis at higher concentrations. My experimental evidence also supports regulation of endogenous PARP-1 expression by the fragment in the absence of DNA damage. This construct has allowed for the visualisation of its functional ability to sensitise cells to oxidative damage and induce apoptosis as observed by the formation of apoptotic precursors and caspase cleavage products in live cells. The data also provides direct evidence for its therapeutic potential in chemotherapy or radiotherapy to avert necrosis induced inflammatory response.

Keywords: Poly (ADP-ribose); Apoptosis; PARP-1 inhibition; DNA repair; DNA binding domain

Introduction

PARP family consists of 17 enzymes but only PARP-1, 2, 3 and 5 are involved in DNA damage response [1]. PARP-1 is an abundant nuclear enzyme activated by DNA breaks and contributes to approximately 85% of cellular PARP activity [2-5]. It has an amino terminal DNA Binding Domain (DBD), central auto modification domain and carboxy terminal catalytic domain. DBD has two Cys-Cys-His-Cys zinc finger motifs (FI and FII) that are involved in DNA binding and nuclear localization signal (NLS). During apoptosis it is cleaved by caspases to 24kDa DBD and 89 kDa catalytic fragments [6].

Reactive Oxygen Species (ROS) such as superoxide anion ($O_2^{\bullet-}$), H_2O_2, hydroxyl radical ($^{\bullet}OH$) and peroxynitrite generated during oxidative stress damage proteins, nucleic acids and cell membranes. All have been implicated in cancer, aging and several neurodegenerative diseases [7-9]. ROS produce DNA lesions leading to activation of repair mechanisms such as Base Excision Repair (BER), Nucleotide Excision Repair (NER) and Recombination Repair (RR). BER in PARP-1 $^{-/-}$ cells is impaired indicating that PARP-1 participates in initiating BER [10,11]. The zinc-finger motifs of PARP-1 DBD bind with high affinity to DNA breaks resulting in the catalytic activation of PARP-1 [12,13]. Activated PARP-1 polymerises linear or branched poly (ADP-ribose) units from NAD+ on numerous target proteins including PARP-1 itself [14]. Binding of PARP-1 to damaged DNA silences transcription and subsequent release of modified PARP-1 initiates repair process. Cell cycle stops at G1 or G2 phase to allow enzymes to repair the damage. Continuous activation of PARP-1 can lead to depletion of NAD+ and ATP and result in cell death [15]. If damage is irreversible cells avoid DNA repair and initiate the apoptotic programme [16]. During apoptosis death ligands bind to and activate TNF-α and Fas receptors. This is followed by activation of caspases, which are critical players in the execution of apoptosis. Caspases activate the DNA fragmentation factor (DFF/ICAD), which degrades chromatin DNA into characteristic 180-200bp fragments. Other features during apoptosis include condensation of chromatin, cell blebbing (nicknamed as "dance of death") due to cytoskeletal weakening around the cell and nuclei and cell shrinkage. Cell shrinkage and membrane blebbing have been described as the earliest and most obvious aspects of apoptotic cell death [17]. PARP-1 is one of the earliest substrates to be cleaved and cleavage by caspases is considered to be a hallmark of apoptosis. Cleavage occurs at the conserved sequence DEVD-/G between Asp214 and Gly215 generating an 89 kDa C-terminal catalytic fragment and a 24 kDa N-terminal fragment [18,19].

The aim of this study was to examine the effect of oxidative damage on poly(ADP-ribose) synthesis and cell morphology in cells expressing different levels of N-terminal fragment of PARP-1. In order to visualise the effects in live cells using confocal laser scanning microscopy this fragment was fused to EGFP and transiently or stably expressed in IRK cells.

Materials

All the chemicals used in this study were of analytical grade. The primers were from Genset. pEGFPN1 and pGEMT-Easy were from Clontech and Promega respectively. Vent DNA polymerase and T4

***Corresponding author:** Dr Ida Rachel Rajiah, Department of Pathology, University of Cambridge, Tennis Court Road, Cambridge CB2 1QP, UK, Tel: +44(0)1223761654; Fax: +44-(0)1223-333346; E-mail: irr23@cam.ac.uk, idarajiah@yahoo.co.uk

Received February 19, 2013; **Accepted** March 20, 2013; **Published** March 22, 2013

Citation: Rajiah IR (2013) PARP-1 N-Terminal Fragment Down-regulates Endogenous PARP-1 Expression and Activity and Sensitises Cells to Oxidative Stress. J Cell Sci Ther 4: 138. doi:10.4172/2157-7013.1000138

DNA Ligase were from New England Biolabs. *Bam*H I was from Gibco BRL, *Hin*d III and calf intestinal alkaline phosphatase were from Roche Diagnostics Ltd. pTG PARP was a kind gift from Dr G de Murcia. Maxi prep kit and DNA purification kit were from Qiagen and Qbiogene-Alexis Ltd respectively. *E.coli* DH5α strain was obtained from Gibco-BRL. IRK cells, a rat embryo fibroblast cell line derived from a Fischer rat embryo was a kind gift from Professor S Shall, Kings College, London.

Designing primers for PCR

The fragment consisting of 750 base pairs or 250 amino acids from the N-terminal end of human PARP-1 was synthesised by PCR using forward and reverse primers, pTGPARP-1 and Vent DNA polymerase. The forward primer consists of 33 bases

5'-ACAACTGCAGGGATCCATGGCGGAGTCTTCGGAT-3'with *Bam*H I and *Pst* I restriction enzyme sites. Reverse primer consists of 44 bases with *Bam*H I and *Xma* I restriction sites 3'GACTAGACCTT-GTAGTTCCTGCCCCTAGGACGGGCCCTAAC-5'.

DNA analysis by agarose gel electrophoresis

Electrophoresis was carried out in 1% or 2% gels and the bands were visualised under UV light using a transilluminator (UVP, Inc., Cambridge, UK). Gels were photographed with a camera and graphic printer (SONY, UP-890CE, Cambridge, UK). DNA was isolated from the gel using BIO 101 geneclean DNA purification kit.

Cloning PCR products into pEGFP

PCR product was first cloned into PGEM-T Easy vector according to the instruction manual from Promega. PARP-1-250 insert was then excised out using *Bam*HI and ligated into *Bam*HI digested pEGFPN1 vector using T_4 DNA ligase. The orientation of the insert was checked using *Hin*d III and the DNA sequence of the construct was verified.

Transient and stable transfection

Large scale preparations of the DNA were made using the maxiprep kit. DNA was introduced into IRK cells using the Gene Pulser from Biorad as described in the instruction manual. Cells were resuspended in complete DMEM and plated on coverslips. Stable transfectants were selected using G418 (500 µg/ml final concentration). Cells on coverslips were washed with PBS-A and mounted onto glass slides for imaging. paraformaldehyde 4% (v/v) and Triton X-100 0.2% (w/v) at room temperature were used for fixing and permeabilisation respectively.

Treatment with hydrogen peroxide

PARP-1 N-term-EGFP transfected cells on coverslips were treated with 0, 50, 100 or 200 µM H_2O_2 (v/v) in PBS-A (final concentration) for 5 minutes at 37°C. Cells were then washed with PBS-A, fixed and permeabilised and mounted onto glass slides. PARP-1 response to oxidative damage in control and PARP-1 N-term-EGFP expressing rodent cells indicated by polymer formation was detected by indirect immunofluorescence using 10H anti-poly (ADP-ribose) primary followed by FITC or Texas Red-conjugated (TXRD) secondary antibodies.

Confocal Laser Scanning Microscopy (CLSM)

Imaging was carried out using Bio-Rad MRC-600 confocal unit (Bio-Rad Laboratories Ltd) that was mounted onto an inverted microscope. EGFP and PARP-1 N-term-EGFP expressing cells were excited at 488 nm with the krypton-argon ion laser line and emission was observed at 510-530 nm. TXRD-labelled specimens were excited at 543 nm with helium-neon ion laser line and emission was observed at 575-630 nm. The laser power, gain and black level were recorded for each experiment and kept constant when comparisons were made. Specimens were viewed and sectioned using an oil immersion × 60 (1.4 numerical aperture) objective lens. Optical sections were taken at 0.8 µm intervals and images collected by Kalman filtering of six scans. For PARP-1 N-term-EGFP and polymer colocalisation studies images were acquired sequentially. False green and red colours were added to PARP-1 N-term-EGFP and polymer respectively and images were merged. Images were analysed using NIH ImageJ software.

Western blotting analysis

Whole cell protein extracts were separated by 8% SDS PAGE and transferred onto nitrocellulose membrane using Transblot apparatus [20]. The membrane was incubated with anti-poly (ADP-ribose) polymerase-1 C-2-10 primary and peroxidase-conjugated secondary antibody. Bands were detected using chemiluminescence luminol reagent and visualised by exposure to X-ray film.

Results

Construction of GFP tagged PARP-1 N-terminal fragment

PARP-1-N-terminal fragment was synthesised by PCR using forward and reverse primers (Figure 1A). Since pGEM-T Easy vector allowed direct cloning without enzymatic manipulation to generate restriction sites the fragment was first cloned into pGEM-T Easy. PARP-1 fragment was then excised out using *Bam*H I and cloned into *Bam*H I digested and dephosphorylated pEGFPN1 as indicated in the vector map (Figure 1B). The ligated plasmid was checked by *Bam*H I digestion and analysed on agarose gel together with 1 kb DNA ladders. Two bands at 4700 bp and 750 bp corresponding to EGFPN1 vector and

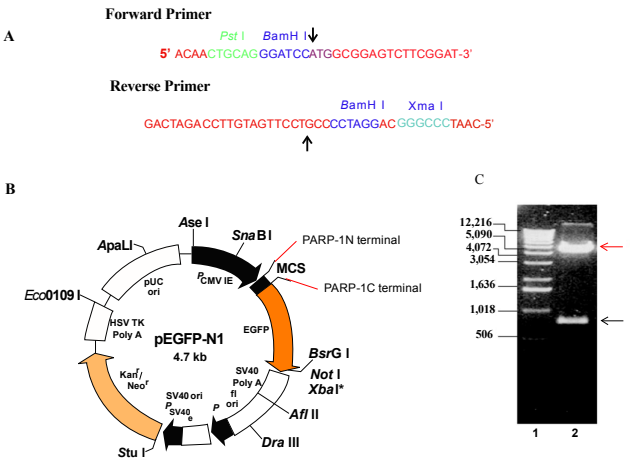

Figure 1: PCR synthesis of PARP-1 N-terminal fragment and cloning into pEGFPN1 vector

A. Forward primer with PstI and BamHI restriction sites and reverse primer with BamHI and XmaI restriction sites were synthesised by Genset. Arrows in the forward and reverse primers indicate PARP-1 start and PARP-1-250 end site respectively. **B**. pEGFP vector map taken from Clontech literature is modified to show PARP-1 fragment N-terminal and C-terminal sites. **C.** PARP-1-N-terminal fragment was cloned into pEGFPN1 vector and digested with BamH1. Digestion products were analysed by agarose gel electrophoresis with 1kb DNA ladder. Red and black arrows indicate bands corresponding to pEGFPN1 vector at 4700 bp and PARP-1-N-terminal fragment at 750 bp respectively. Data shown is representative of three separate experiments.

PARP-1-N-terminal fragment respectively indicated successful ligation (Figure 1C). The insert was checked for correct orientation using *Hin*d III. Sequencing data showed that it was in frame with the EGFP coding sequence and did not contain any intervening stop codons. The amino acid sequence showed 100% identity with human PARP-1.

PARP-1 N-terminal fragment is distributed differentially during interphase and mitosis

Full length PARP-1 tagged to DsRed or EYFP and 24kDa N-terminal fragment tagged to pDsRed-N1 are present in the nucleoli and nucleoplasm of live COS-7 and HeLa S3 cells [21]. Electron microscopic images of fixed HeLa cells show full-length PARP-1 staining over the entire chromatin with greater intensity of staining closer to the nuclear membrane and the interchromatin space devoid of staining [22]. However a detailed study of PARP-1 N-terminal fragment localisation during interphase and mitosis within live cells has not been reported. During interphase of the cell cycle PARP-1-N-term-EGFP was found exclusively in the nuclei of live IRK cells transiently or stably expressing the protein. The positive control, EGFP vector was present through-out the whole cell (Figure 2A Panels 1-4). Detailed analysis of the nuclei by CLSM revealed a continuous distribution of the protein along the nuclear periphery and as patches within the central region (Figure 2A, Panels 5 and 6). Optical Z stacks of images revealed localisation of the fragment in the mid-sections of the nucleus (Figure 2B).

Actively growing cells were examined live for distribution of the tagged protein at different stages of mitosis (Figure 2C). During Prophase, aggregates of the fusion protein were seen within the nucleus and along the nuclear membrane; at prometaphase dense strands were distributed through-out the cell. At metaphase these dense strands were seen at the equatorial region. During anaphase, two separate groups of dense strands, 5-6µm apart was present at early telophase and two dense patches against a moderately fluorescent background at telophase. Hence through-out mitosis PARP-1-N-term-EGFP was associated with the chromatin. Furthermore there is equal distribution of the protein in the daughter cells.

Exogenous PARP fragment regulates endogenous PARP-1 activity and induces apoptosis

In vivo studies show that over expression of PARP-1-DBD inhibits endogenous PARP-1 activity in mouse fibroblasts [23]. But the effect of different concentrations of H_2O_2 on polymer synthesis in cells expressing different levels of this domain has not been explored. IRK cells stably expressing EGFP tagged PARP-1-N-terminal fragment were treated with different concentrations of H_2O_2 and polymer synthesis was examined by CLSM. At 50 µM H_2O_2 fusion protein expression without polymer synthesis was detected in 45% of cells and polymer synthesis without fusion protein expression was detected in 32% of cells. At 100 µM H_2O_2 14% of cells displayed both (Figures 3A and 3B). No polymer synthesis was observed in untreated, transfected control cells (Figure 3B Panel 1). Non-transfected cells subjected to identical treatment showed polymer synthesis in all the cells at 50 and 100 µM H_2O_2 although the intensity of staining was higher at 100 µM (Figure 3B Panels 4-6). Cells presenting both fusion protein expression and polymer synthesis were examined at high magnification. They were categorised into cells displaying high, medium and low levels of fluorescence (Figure 3C). Comparison of mean fluorescence intensities of fusion protein expression (green) and polymer synthesis (red) showed significant reduction in polymer synthesis in high and medium expressing cells (Figure 3D). Although in the low expressing cells MFI of polymer staining was relatively higher it was 40% less than non-transfected, 100 µM H_2O_2 treated control cells. PCC values indicated no colocalisation. Hence it was evident that polymer synthesis occurred in areas devoid of fusion protein expression.

HeLa cells stably expressing PARP-1-DBD and treated with N-methyl-N'-nitro-N-nitrosoguanidine (MNNG) show nucleosomal DNA ladder formation, one of the hallmarks of cell death by apoptosis [24]. I investigated the morphological changes in live cells following oxidative damage in the presence of exogenous PARP-1-N-terminal fragment. At 200 µM H_2O_2 treatment, fluorescence was observed exclusively in the nucleus within 4% of cells and exclusively in the cytoplasm in 58% and fluorescence was observed both in nucleus and cytoplasm in 9% cells (Figure 4A Panel 1, 4B). At high magnification nuclear membrane presented a notched or uneven morphology (Figure 4C, Panels 2, 3 and 4). Untreated, control cells expressing the fusion protein showed fluorescence exclusively in the nucleus with a smooth

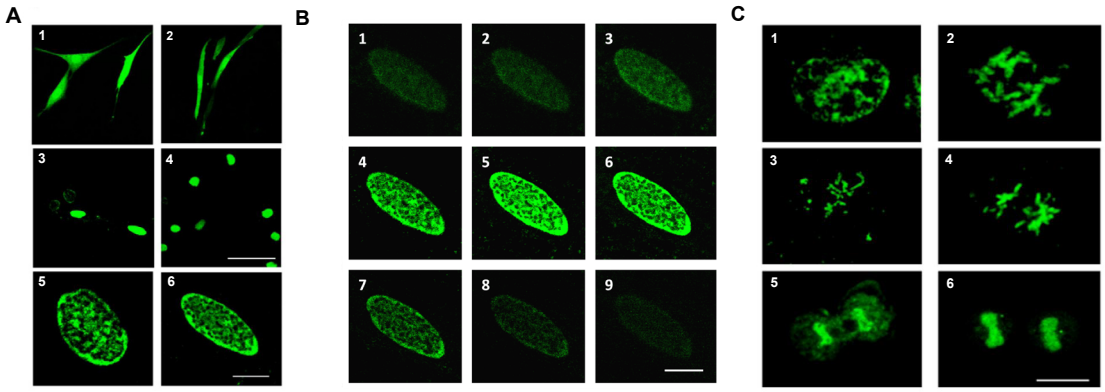

Figure 2: PARP-1-N-term-EGFP localisation in live cells during interphase and mitosis

PARP-1-N-term-EGFP construct was introduced into IRK cells by electroporation. After 24 hours live cells were examined using confocal laser scanning microscopy. **A.** Panels 1 and 2, cells expressing EGFP plasmid (control). Panels 3 and 4, cells expressing PARP-1 N-term-EGFP. Scale bar represents 75 µm. Panels 5 and 6, nuclei of cells in interphase expressing PARP-1 N-term-EGFP. Scale bar represents 10 µm. **B.** Optical sections of Z stack collected at 0.8 µm interval. **C.** Mitotic cells expressing PARP-1 N-term-EGFP. Panels 1-6 are prophase, prometaphase, metaphase, anaphase, early telophase and telophase respectively. Scale bar for B and C represents 10 µm. Each panel is representative of at least 60 cells from three separate transfections.

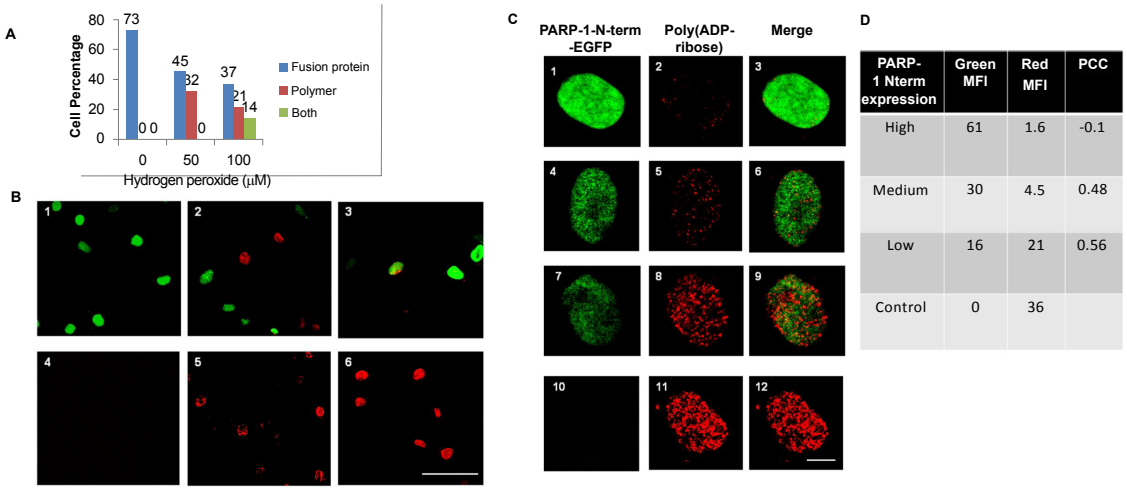

Figure 3: Poly(ADP-ribose) synthesis is inhibited in cells expressing PARP-1-N-term-EGFP

IRK cells stably expressing PARP-1-N-term-EGFP treated with different concentrations of hydrogen peroxide for 5 minutes, fixed, permeabilised and stained for poly(ADP-ribose) using 10H primary antibody and Texas-red conjugated secondary antibody. **A.** Percentage of cells expressing fusion protein, polymer staining or both. **B.** Panels 1, 2 and 3, merged images of fusion protein and polymer staining in cells treated with 0, 50 and 100 μM hydrogen peroxide respectively. Panels 4, 5 and 6, Non-transfected cells subjected to identical treatment and stained for poly(ADP-ribose). Scale bar represents 75 μm. **C**. Panels 1-9, Nuclei of cells presenting PARP-1-N-term-EGFP expression and polymer synthesis at high magnification. Panel 10-12, non-transfected cell treated with 100 μM hydrogen peroxide (control). Scale bar represents 6 μm. Each panel is representative of at least 60 cells from three separate experiments. **D**. Mean fluorescence intensities (MFI) of fusion protein and polymer in cells expressing high, medium and low levels of fusion protein. Data is representative of at east 100 cells from three separate experiments.

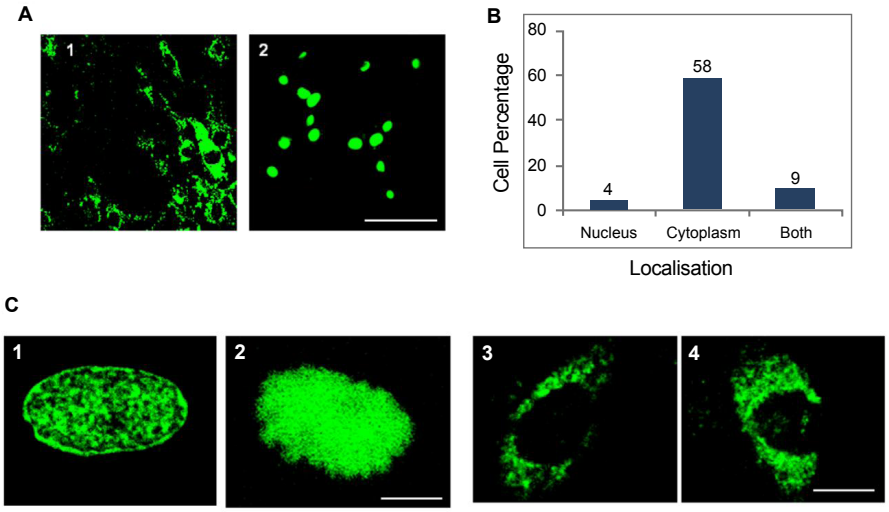

Figure 4: PARP-1-N-term-EGFP expressing cells treated with 200 μM hydrogen peroxide undergo apoptosis

A. Panel 1, IRK cells expressing PARP-1 N-term-EGFP treated with 200 μM hydrogen peroxide for 5 minutes and examined live by CLSM. Panel 2, Non-transfected IRK cells treated with 200 μM hydrogen peroxide for 5 minutes, fixed, permeablised and stained for poly (ADP-ribose) using 10H primary antibody and FITC conjugated secondary antibody. Scale bar represents 75 μm. **B.** Localisation of fusion protein following treatment with 200 μM hydrogen peroxide **C.** Panel 1, nucleus of untreated cell expressing PARP-1 N-term-EGFP. Panel 2, Nucleus of cell displaying membrane blebbing. Scale bar represents 6 μm. Panels 3 and 4, cells showing fluorescence in cytoplasm. Scale bar represents 22 μm. Each panel is representative of at least 60 cells from three separate experiments.

and even nuclear membrane (Figure 4C, Panel 1). Non-transfected cells subjected to identical treatment with H_2O_2 and probed for polymer synthesis confirmed endogenous PARP-1 activation and also presented smooth nuclear membranes (Figure 4A, Panel 2).

Exogenous PARP-1-N-terminal fragment inhibits endogenous PARP-1 expression

According to Yung et al. [25], Western blotting analysis of COS-7 cells transfected with EYFP or DsRed tagged full-length PARP-1 shows identical levels of the tagged and endogenous PARP-1 protein. Moreover endogenous PARP-1 expression is identical in non-transfected and transfected samples. I explored the effect of the N-terminal fragment on endogenous PARP-1 expression. Extracts of transiently transfected and non-transfected control IRK cells, together with wide molecular weight range protein standards were subjected to Western blotting. They were probed with antiPARP-1 antibody, (raised against a synthetic peptide corresponding to amino acids 2-20 at the N-terminal of human PARP-1) followed by peroxidase-conjugated secondary antibody.

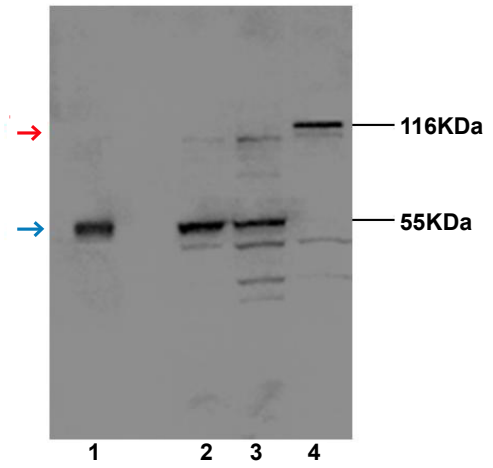

Figure 5: Endogenous PARP-1 expression is reduced in cells expressing PARP-1 N-term-EGFP

IRK cells were electroporated with PARP-1-N-term-pEGFP. Cell extracts were prepared at different times after electroporation and analysed by Western blot using antiPARP-1 antibody (raised against a synthetic peptide corresponding to amino acids 2-20 at the N-terminal of PARP-1) followed by peroxidase-conjugated secondary antibody. Lane 1, 24 hours, Lane 2, 48 hours, Lane 3, 72 hours. Lane 4, Non-transfected IRK cell extract (control). Red and blue arrows indicate endogenous PARP-1 and PARP-1-N-term-EGFP bands at 116 kDa and 55 kDa respectively. Data is representative of three separate experiments.

Immunoreactivity at 55kDa corresponding to the predicted molecular weight of PARP-1 N-term-EGFP (calculated molecular weight, 56kDa) was very strong in all the transiently transfected samples but no reactivity in the control IRK sample (Figure 5). At 116 kDa corresponding to full length PARP-1, immunoreactivity was undetectable in the 24, 48 and 72 hour transiently transfected samples and strong reactivity in the control IRK sample. Very weak reactivity to cleavage products of endogenous PARP-1 was seen in 48, 72 hour and control samples. From this data it was clearly evident that endogenous PARP-1 was significantly reduced by the expression of the N-terminal fragment.

Discussion

The subnuclear distribution of PARP-1 in fixed HeLa and mouse embryonic fibroblast cells shows a granular pattern with areas of strong intensity [26]. Using live cell imaging I have shown the distribution of the N-terminal fragment in the nuclear periphery. I have also shown in live cells that this fragment is associated with the chromatin throughout mitosis and equally distributed in the daughter cells. This finding suggests that this domain of PARP-1 is an integral part of the mitotic machinery and involved in DNA damage surveillance network during interphase and mitotic phases of the cell cycle. Furthermore, following cell division there is symmetrical segregation of the protein in the daughter cells.

My study has highlighted the effects of different levels of fusion protein expression on polymer synthesis. A 40% reduction in polymer synthesis was observed following oxidative damage in cells expressing the fusion protein with an average MFI of 16 (Figure 3D). It has been reported by Yung and Satoh that in the presence of an 8-fold excess of the N-terminal fragment there was a 50% drop in polymer synthesis [27]. Hence in accordance with previous reports my fusion protein is functionally a potent trans-dominant inhibitor of BER. Adherent cultured cells treated with moderate levels of H_2O_2 display blebbing due to weakening of the cell membrane, rounding-up, and detachment from the growth surface [28-30]. My data has provided evidence for the first time blebbing or notching of the nuclear membrane indicating that it could be a precursor to apoptotic body formation (Figure 4C, panel 2). During apoptosis PARP-1 is one of the first substrates to be cleaved and inactivated by proteases. Since the NLS encompasses the caspase cleavage site it was possible to visualise this effect by confocal imaging. In Figure 4C, panels 3 and 4, apoptotic cleavage of the fusion protein and loss of NLS had resulted in the translocation of the GFP-tagged cleaved fragment from the nucleus to cytoplasm.

PARP-DBD acts as a dominant-negative mutant by binding to DNA strand breaks irreversibly and sensitising cells to DNA-damaging agents [31,32]. It is evident from my data that exogenous PARP-1-N-terminal fragment had sensitised cells to 200μM H_2O_2 treatment because untransfected cells subjected to similar treatment did not show signs of apoptosis. Consequently, PARP-1 is cleaved which in turn promotes apoptosis and averts necrotic cell death or energy depleting cell survival. Indeed this data is consistent with the model by D'amours et al. where PARP cleavage averts energy-depletion induced necrotic cell death [23]. Prior to this it was reported that in the presence of moderate levels of DNA damage cells expressing uncleavable PARP-1 shift their mode of cell death from apoptosis to necrosis [33]. My findings also show that the N-terminal fragment represses endogenous PARP-1 expression in untreated cells. Soldatenkov et al. has shown *in vivo* that full-length PARP-1 protein binds to the 5' flanking region of the human PARP-1 gene promoter from Ewing's sarcoma cells and inhibits PARP-1 expression [34]. However, my data indicates that exogenous expression of the N-terminal fragment is sufficient to cause this inhibition.

In summary this study has provided an insight into the localisation of the N-terminal fragment of human PARP-1 during interphase and mitosis and also the functional and cytological changes that follow oxidative damage in live cells. IRK cells expressing the tagged protein are functionally identical to control IRK cells and catalyse poly (ADP-ribose) in response to oxidative damage. However, they show reduced endogenous PARP-1 activity and they are more susceptible to apoptosis compared to non-transfected cells. Furthermore, in the absence of oxidative stress the fragment functions as a negative regulator of PARP-1 expression. Hence in addition to playing a major role in the surveillance of DNA breaks the N-terminal fragment can also regulate PARP-1 expression. My construct is a biological inhibitor of endogenous PARP-1 and owing to its ability to sensitise cells to oxidative damage it will serve as a powerful supplement for treatment of tumours by chemotherapy and radiotherapy. Due to its ability to bind to DNA breaks irreversibly and inhibit polymer synthesis this fragment would be more potent than chemical inhibitors that act by competing with the substrate.

Acknowledgements

I would like to thank Dr Minnie O'Farrell, Retired Lecturer, Department of Biological Sciences, University of Essex, Colchester CO4 3SQ, England for conception of the project, Dr Peter Alefounder for assistance with designing PARP-1-N-term-EGFP construct and Jeremy Skepper, Technical Director MIC, Anatomy Building, PDN, University of Cambridge, Tennis Court Road, Cambridge CB2 1QP, England for valuable comments. This research work was self-funded.

References

1. Amé JC, Spenlehauer C, de Murcia G (2004) The PARP superfamily. Bioessays 26: 882-893.
2. Boulikas T (1991) Relation between carcinogenesis, chromatin structure and poly(ADP-ribosylation) (review). Anticancer Res 11: 489-527.
3. Yamanaka H, Penning CA, Willis EH, Wasson DB, Carson DA, et al. (1988)

Characterization of human poly(ADP-ribose) polymerase with autoantibodies. J Biol Chem 263: 3879-3883.

4. Woodhouse BC, Dianov GL (2008) Poly ADP-ribose polymerase-1: An international molecule of mystery. DNA Repair (Amst) 7: 1077-1086.
5. D'Amours D, Desnoyers S, D'Silva I, Poirier GG (1999) Poly(ADP-ribosyl)ation reactions in the regulation of nuclear functions. Biochem J 342: 249-268.
6. Schreiber V, Dantzer F, Ame JC, de Murcia G (2006) Poly(ADP-ribose): Novel functions for an old molecule. Nat Rev Mol Cell Biol 7: 517-28.
7. Sastre J, Pallardo FV, Vina J (2000) Mitochondrial oxidative stress plays a key role in aging and apoptosis. IUBMB Life 49: 427-435.
8. Sayre LM, Smith MA, Perry G (2001) Chemistry and biochemistry of oxidative stress in neurodegenerative disease. Curr Med Chem 8: 721-738.
9. Valko M, Izakovic M, Mazur M, Rhodes CJ, Telser J, et al. (2004) Role of oxygen radicals in DNA damage and cancer incidence. Mol Cell Biochem 266: 37-56.
10. Dantzer F, de La Rubia G, Menissier-De Murcia J, Hostomsky Z, de Murcia G, et al. (2000) Base excision repair is impaired in mammalian cells lacking Poly(ADP-ribose) polymerase-1. Biochemistry 39: 7559-7569.
11. Dantzer F, Schreiber V, Niedergang C, Trucco C, Flatter E, et al. (1999) Involvement of poly(ADP-ribose) polymerase in base excision repair. Biochimie 81: 69-75.
12. Gille JJ, Joenje H (1992) Cell culture models for oxidative stress: superoxide and hydrogen peroxide versus normobaric hyperoxia. Mutat Res 275: 405-414.
13. de Murcia G, Menissier-de Murcia J, Schreiber V (1991) Poly(ADP-ribose) polymerase: molecular biological aspects. Bioessays 13: 455-462.
14. Cox LS, Lane DP (1995) Tumour suppressors, kinases and clamps: how p53 regulates the cell cycle in response to DNA damage. Bioessays 17: 501-508.
15. Nosseri C, Coppola S, Ghibelli L (1994) Possible involvement of poly(ADP-ribosyl) polymerase in triggering stress-induced apoptosis. Exp Cell Res 212: 367-373.
16. Mocali A, Caldini R, Chevanne M, Paoletti F (1995) Induction, effects, and quantification of sublethal oxidative stress by hydrogen peroxide on cultured human fibroblasts. Exp Cell Res 216: 388-395.
17. Kerr JF, Wyllie AH, Currie AR (1972) Apoptosis: a basic biological phenomenon with wide-ranging implications in tissue kinetics. Br J Cancer 26: 239-257.
18. Kaufmann SH, Desnoyers S, Ottaviano Y, Davidson NE, Poirier GG (1993) Specific proteolytic cleavage of poly(ADP-ribose) polymerase: an early marker of chemotherapy-induced apoptosis. Cancer Res 53: 3976-3985.
19. Tewari M, Quan LT, O'Rourke K, Desnoyers S, Zeng Z, et al. (1995) Yama/CPP32 beta, a mammalian homolog of CED-3, is a CrmA inhibitable protease that cleaves the death substrate poly(ADP-ribose) polymerase. Cell 81: 801-809.
20. Laemmli UK (1970) Cleavage of structural proteins during the assembly of the head of bacteriophage T4. Nature 27: 680-685.
21. Smulson ME, Pang D, Jung M, Dimtchev A, Chasovskikh S, et al. (1998) Irreversible binding of poly(ADP)ribose polymerase cleavage product to DNA ends revealed by atomic force microscopy: possible role in apoptosis. Cancer Res 58: 3495-3498.
22. Yung TM, Satoh MS (2001) Functional competition between poly(ADP-ribose) polymerase and its 24-kDa apoptotic fragment in DNA repair and transcription. J Biol Chem 276: 11279-11286.
23. D'Amours D, Sallmann FR, Dixit VM, Poirier GG (2001) Gain-of-function of poly(ADP-ribose) polymerase-1 upon cleavage by apoptotic proteases: implications for apoptosis. J Cell Sci 114: 3771-3778.
24. Schreiber V, Hunting D, Trucco C, Gowans B, Grunwald D, et al. (1995) A dominant-negative mutant of human poly(ADP-ribose) polymerase affects cell recovery, apoptosis, and sister chromatid exchange following DNA damage. Proc Natl Acad Sci U S A 92: 4753-4757.
25. Yung TM, Sato S, Satoh MS (2004) Poly(ADP-ribosyl)ation as a DNA damage-induced post-translational modification regulating poly(ADP-ribose) polymerase-1-topoisomerase I interaction. J Biol Chem 279: 39686-39696.
26. Meder VS, Boeglin M, de Murcia G, Schreiber V (2005) PARP-1 and PARP-2 interact with nucleophosmin/B23 and accumulate in transcriptionally active nucleoli. J Cell Sci 118: 211-222.
27. Yung TM, Satoh MS (2001) Functional competition between poly(ADP-ribose) polymerase and its 24-kDa apoptotic fragment in DNA repair and transcription. J Biol Chem 276: 11279-11286.
28. Bellomo G, Jewell SA, Thor H, Orrenius S (1982) Regulation of intracellular calcium compartmentation: studies with isolated hepatocytes and t-butyl hydroperoxide. Proc Natl Acad Sci U S A 79: 6842-6846.
29. Thornberry NA, Lazebnik Y (1998) Caspases: enemies within. Science 281: 1312-1316.
30. Zimmermann KC, Green DR (2001) How cells die: apoptosis pathways. J Allergy Clin Immunol 108: S99-S103.
31. Kupper JH, de Murcia G, Burkle A (1990) Inhibition of poly(ADP-ribosyl)ation by overexpressing the poly(ADP-ribose) polymerase DNA-binding domain in mammalian cells. J Biol Chem 265: 18721-18724.
32. Molinete M, Vermeulen W, Burkle A, Menissier-de Murcia J, Kupper JH, et al. (1993) Overproduction of the poly(ADP-ribose) polymerase DNA-binding domain blocks alkylation-induced DNA repair synthesis in mammalian cells. EMBO J 12: 2109-2117.
33. Kim JW, Won J, Sohn S, Joe CO (2000) DNA-binding activity of the N-terminal cleavage product of poly(ADP-ribose) polymerase is required for UV mediated apoptosis. J Cell Sci 113: 955-961.
34. Soldatenkov VA, Chasovskikh S, Potaman VN, Trofimova I, Smulson ME, et al. (2002) Transcriptional repression by binding of poly(ADP-ribose) polymerase to promoter sequences. J Biol Chem 277: 665-670.